The Journal of Experimental Biology 211, 3323-3332
Published by The Company of Biologists 2008
doi:10.1242/jeb.018887

Blood flow and metabolic regulation in seal muscle during apnea

Paul J. Ponganis[1], Ulrike Kreutzer[2], Torre K. Stockard[1], Ping-Chang Lin[2], Napapon Sailasuta[3], Tuan-Khan Tran[2], Ralph Hurd[3] and Thomas Jue[2,*]

[1]Center for Marine Biotechnology and Biomedicine, Scripps Institution of Oceanography, University of California San Diego, La Jolla, CA 92093, USA, [2]Department of Biochemistry and Molecular Medicine, University of California Davis, Davis, CA 95616, USA and [3]GE Medical Systems, Fremont, CA 94539, USA

*Author for correspondence (e-mail: TJue@ucdavis.edu)

Accepted 19 August 2008

SUMMARY

In order to examine myoglobin (Mb) function and metabolic responses of seal muscle during progressive ischemia and hypoxemia, Mb saturation and high-energy phosphate levels were monitored with NMR spectroscopy during sleep apnea in elephant seals (*Mirounga angustirostris*). Muscle blood flow (MBF) was measured with laser-Doppler flowmetry (LDF). During six, spontaneous, 8–12 min apneas of an unrestrained juvenile seal, apneic MBF decreased to 46±10% of the mean eupneic MBF. By the end of apnea, MBF reached 31±8% of the eupneic value. The $t_{1/2}$ for 90% decline in apneic MBF was 1.9±1.2 min. The initial post-apneic peak in MBF occurred within 0.20±0.04 min after the start of eupnea. NMR measurements revealed that Mb desaturated rapidly from its eupenic resting level to a lower steady state value within 4 min after the onset of apnea at rates between 1.7±1.0 and 3.8±1.5% min^{-1}, which corresponded to a muscle O_2 depletion rate of 1–2.3 ml O_2 kg^{-1} min^{-1}. High-energy phosphate levels did not change with apnea. During the transition from apnea to eupnea, Mb resaturated to 95% of its resting level within the first minute. Despite the high Mb concentration in seal muscle, experiments detected Mb diffusing with a translational diffusion coefficient of 4.5×10^{-7} cm^2 s^{-1}, consistent with the value observed in rat myocardium. Equipoise P_{O_2} analysis revealed that Mb is the predominant intracellular O_2 transporter in elephant seals during eupnea and apnea.

Key words: Doppler, muscle, myoglobin, NMR, oxygen, hemodynamics.

INTRODUCTION

The prolonged breath holds (apneas) of seals during sleep represent a model in which to examine the interplay of vascular O_2 delivery, the MbO_2 (oxymyoglobin) store and cellular metabolic responses during progressive hypoxemia and muscle ischemia. These spontaneous apneas are routinely 7–10 min in duration in northern elephant seals, *Mirougna angustirostris* Gill (Le Boeuf et al., 2000). Both the breath holds and the post-apneic ventilatory periods (eupneas) occur during slow-wave sleep (Castellini et al., 1994; Le Boeuf et al., 2000). These two factors, apneic duration and a sleeping, non-mobile subject, make sleep apnea in the elephant seal a model in which it is feasible to conduct detailed physiological and biochemical investigations.

Physiological and metabolic responses during these sleep apneas contrast with those observed during forced submersions of seals. First, during sleep apnea, a mild bradycardia of 40–50 beats min^{-1} maintains cardiac output at levels characteristic of similarly sized mammals at rest (Andrews et al., 1997; Ponganis et al., 2006). Such moderate bradycardias are also characteristic of many dives (Andrews et al., 1997). Second, mean apneic muscle blood flow (MBF), as measured by laser-Doppler flowmetry (LDF), declines to only 50% of the eupneic level (Ponganis et al., 2006). Third, blood lactate concentrations do not change (Castellini et al., 1986) even as both arterial and venous oxygen partial pressure (P_{O_2}) decline to 15–20 mmHg (1 mmHg=0.133 kPa) by the end of long apneas (Stockard et al., 2007). By contrast, during forced submersions, the animals exhibit severe bradycardia and peripheral vasoconstriction, which isolate muscle and most organs from the circulation and preserve blood O_2 for the brain and heart (Blix et al., 1983; Elsner et al., 1964; Scholander, 1940; Zapol et al., 1979). Under the extreme physiological conditions during forced submersions, muscle metabolism must presumably rely on the large Mb-bound O_2 store, creatine kinase reaction and glycolysis to generate ATP (Scholander, 1940; Scholander et al., 1942; Stephenson and Jones, 1992).

The high Mb concentrations in seal muscle have classically been considered to provide an O_2 store (Scholander, 1940; Scholander et al., 1942). Recently, however, studies have suggested that the Mb in seal muscle serves primarily to facilitate diffusion of O_2 and that blood-to-muscle O_2 transfer accounts for the less than expected Mb desaturation detected with near-infrared spectroscopy (NIRS) during dives (Guyton et al., 1995). Since NIRS cannot distinguish Mb and Hb signals, questions still remain about the role of Mb in regulating O_2 consumption during a breath hold. In addition, on the basis of measurements of Mb translational diffusion coefficients, Mb does not contribute significantly to the O_2 flux in myocyte and perfused rat myocardium (Lin et al., 2007a; Lin et al., 2007b; Papadopoulos et al., 2001). Therefore, further investigations of seal muscle are necessary in order to better define the muscle metabolic responses and the role(s) of the exceptionally high Mb concentrations in these divers.

In contrast to NIRS, ^{1}H NMR techniques can discriminate the deoxy-Mb and deoxy-Hb proximal histidyl $N_\delta H$ signals *in vivo*. These signals reflect the change in tissue and vascular P_{O_2}. As P_{O_2} falls, the proximal histidyl $N_\delta H$ signal of deoxy-Mb and deoxy-Hb signal intensity increases (Kreutzer et al., 1992; Ponganis et al., 2002; Tran et al., 1999). These peaks yield a quantitative measurement of dynamic changes in the intracellular and vascular oxygenation during a breath hold (Chung et al., 2005; Jue, 2004; Kreutzer and Jue, 1995; Kreutzer et al., 1998; Tran et al., 1999). In addition, NMR

techniques allow the calculation of Mb translational diffusion coefficients (Lin et al., 2007a; Lin et al., 2007b). The present study has applied NMR spectroscopy in combination with LDF to evaluate cellular metabolic responses of seal muscle to the progressive ischemia and hypoxemia of sleep apnea.

Indeed, MbO_2 desaturates approximately 20% from its control level during apnea and resaturates rapidly at the beginning of eupnea. The Mb and MBF kinetics correlate and suggest a local vasoconstriction mechanism. Moreover, the translational diffusion measurements demonstrate that Mb has a predominant role in facilitating O_2 diffusion under all physiological conditions. Mb releases part of its O_2 store at the beginning of apnea. The blood-to-cell O_2 gradient narrows as apnea progresses and implicates a relative reduction in energy metabolism during late apnea in comparison with eupnea and the start of apnea. The present study establishes the experimental basis to study the metabolic adaptations associated with sleep apnea in seals (Ponganis et al., 2002).

MATERIALS AND METHODS

Animal preparation

Juvenile northern elephant seals (*Mirounga angustirostris*; 62–73 kg) were obtained from Sea World of San Diego's Rehabilitation Program, San Diego, CA, USA, and were maintained at the tank facility at Scripps Institution of Oceanography. They were fed smelt, 5–10% of their body mass per day, supplemented with daily vitamins and were released to sea off San Diego after completion of these studies. The seals had been found beached after their first trip to sea, were rehabilitated at Sea World and were judged to be healthy by the Sea World staff.

Two eight-month old seals (70 and 62 kg in body mass) were used for the NMR studies. They were transported by van to the University of California San Francisco (UCSF), CA, USA. *En route*, they were maintained at the University of California Santa Cruz (UCSC) Long Marine Laboratory, Santa Cruz, CA, USA. The 70 kg seal was also used in the blood flow studies.

This research protocol was approved by the UCSD, UCSC and UCSF Animal Subjects Committees and was conducted under a marine mammal permit (#732-1487).

Blood flow

The LDF measurements were conducted as described previously (Ponganis et al., 2006). Briefly, after intramuscular ketamine (2 mg kg^{-1}) sedation, a fiberoptic LDF probe (Transonics N Type probe, ALF 21 flowmeter, Ithaca, NY, USA) was placed percutaneously under local anesthesia (2% xylocaine, intradermal) into the longissimus dorsi muscle (5 cm depth). The probe was secured to the skin with a neoprene patch and epoxy glue. After recovery from anesthesia (4 h), the unrestrained 70 kg seal exhibited spontaneous, 4–10 min apneas during periods in which the seal appeared somnolent and exhibited the occasional facial twitching characteristic of sleep apnea (Castellini et al., 1994). Blood flow was recorded on a personal computer at 100 Hz frequency with Axotape (Axon Instruments, Foster City, CA, USA) software. Visual or auditory monitoring of respirations allowed event marking on the recording system. Instantaneous beat-to-beat heart rate (f_H) and flow were calculated and verified with Acqnowledge software (Biopac Systems, Santa Barbara, CA, USA). Blood flow profiles were constructed on Origin 4.1. Apneic and eupneic MBFs were defined as the flow rate measured during the entire apneic or eupneic period.

The flow probe was removed after ketamine sedation. Prophylactic cefalexin was administered intravenously (1 g) on the day of the study and for two days afterwards (250 mg per orem, three times per day). Zero flow calibration of the probe was conducted by inserting the probe into the longissimus dorsi muscle of an elephant seal carcass and resulted in a value of 0.03±0.02 perfusion units (mean ± s.d.). Percutaneous needle muscle biopsy samples were also obtained after ketamine sedation (Ponganis et al., 1993b).

In vivo NMR

In vivo NMR measurements were performed on a 1 m bore diameter GE Signa scanner (GE Medical Systems, Fremont, CA, USA) at 1.5 T using the same seal used in the MBF study. In San Diego, the seal was trained to enter a fiberglass tube, which was fitted to the magnet bore and in which the unrestrained seal exhibited spontaneous sleep apnea episodes. After the seal's entry into the tube at UCSF, the tube containing the seal was placed into the scanner for the study. During the NMR experiments, an experienced observer monitored the seal's breathing pattern and signaled to the investigators in the adjacent control room when the seal took a breath. The breathing pattern was noted and then cross-referenced to a timer as well as to the NMR signal acquisition data block.

^{1}H (63.86 MHz) NMR signal acquisition utilized a body coil transmit/surface coil (13 cm diameter) receive configuration (Ponganis et al., 2002). The receive coil was positioned over the region of the longissimus dorsi muscle group. Magnetic field shimming was achieved using a three-point Dixon method, yielding a water line-width of approximately 40 Hz (Glover and Schneider, 1991). A modified-DANTE pulse sequence excited the deoxy-Mb His-F8 $N_\delta H$ signals, approximately 4.6 kHz from the water resonance (Morris and Freeman, 1978). Each spectrum required 300 transients and corresponded to a total acquisition time of 60 s.

^{31}P NMR data were collected from a second seal of similar age but only 62 kg in body mass. ^{31}P (25.85 MHz) signal acquisition utilized a conforming flexible coil, which wrapped around the dorsum of the lumbar region. A 50 mm slice was selected and then excited with a self-refocused 45 deg. radio frequency pulse. The effective echo time was set at 2.5 ms. The other acquisition parameters were as follows: spectral width, 2.5 kHz; data points, 2048; acquisition time, 820 ms; recycle time, 2 s. Each ^{31}P NMR spectrum consisted of 25 transients and required a total acquisition time of 70 s. All spectra were apodized with a 15 Hz exponential function and referenced to phosphocreatine (PCr) as 0 p.p.m.

Because the ^{31}P peak line-widths during eupnea and apnea did not vary, the analysis set the most intense PCr peak during eupnea as 100%. The relative change in PCr and ATP concentration during the course of the experiment, as reflected in the signal intensity of PCr at 0 p.p.m. and βATP at –16 p.p.m., used this value as a basis to determine statistical significance.

Data were exported from the Signa system to a Sun Sparc2 workstation and processed using Omega 6.0 software (GE Medical Systems). All spectra were zero filled to 2 k and apodized using a Gaussian-exponential function with a line-broadening of 50 Hz. All spectra were baseline corrected and referenced to water at 4.65 p.p.m.

Mb signal calibration

Analysis of the muscle biopsy sample from the longissimus dorsi muscle yielded a Mb concentration of 4.5 g 100 g^{-1} muscle (Reynafarje, 1963; Ponganis et al., 2002). The deoxy-Mb signal was calibrated against the reference signal from a phantom containing a 100 ml solution of 2 mmol l^{-1} metHb as previously described (Tran et al., 1999). No T_1-based saturation factor correction was necessary

as the T_1s of both the Mb and Hb signals were sufficiently rapid to permit full recovery within the recycle time. Multi-slice images of the seal revealed the surface coil detectable tissue volume and an approximately 3 cm-thick fat layer. Digitally removing the fat contribution from the image yielded an estimate of the muscle volume. The muscle volume, the signal intensity of the phantom metHb solution and the experimentally determined Mb concentration of seal muscle are necessary to determine the percentage change in the deoxy-Mb and deoxy-Hb signal intensity during apnea. As the image analysis overestimates the muscle volume, the percentage change in MbO_2 and HbO_2 desaturation represents an underestimated value.

Tissue temperature

The temperature-dependent chemical shift of the proximal histidyl $N_\delta H$ signal of deoxy-Mb and deoxy-Hb provided a basis to estimate tissue temperature, using a calibration curve derived from the measurement of chemical shift of the $N_\delta H$ signal of pure deoxy-Mb and deoxy-Hb in solution *vs* $1/T$ (Ponganis et al., 2002). The calculation used 14 chemical shift measurements of the deoxy-Mb signal after the intensity had reached a steady state in two representative apnea periods.

Mb diffusion in seal muscle

Measurements of Mb translational diffusion were conducted on a muscle biopsy sample obtained from a juvenile elephant seal. The sample was kept on ice and shipped overnight to University of California Davis. The NMR analysis used portions of the sample immersed in isotonic saline. Upon completion of the measurements, an optical assay of the isotonic solution determined if any Mb had leaked from the tissue (Masuda et al., 2008). None was detected.

An Avance 400 MHz Bruker spectrometer (Billerica, MA, USA) measured the translational diffusion with a 10 mm microimaging gradient probe. The ^{1}H 90 deg. pulse was 17.5 μs. A modified Stejskal–Tanner pulsed-field gradient spin echo (PGSE) sequence followed the Val E11 resonance of MbCO and MbO_2 at –2.4 p.p.m. and –2.8 p.p.m., respectively (Price, 1997; Stejskal and Tanner, 1965). The gradient field strength ranged from 0 to 95 G [gauss cm^{-1} (1 gauss=10^4 tesla)]. A typical spectrum required 1024 scans and used the following signal acquisition parameters: spectral width, 8192 Hz; data points, 4096; acquisition time, 255 ms. The H_2O line served as the spectral reference, 4.75 p.p.m. at 25°C relative to sodium-3-(trimethylsilyl)propionate-2,2,3,3-d4 at 0 p.p.m.

Diffusion measurements in seal muscle tissue experiments utilized a modified PGSE sequence in which a modified 1331 binomial pulse sequence replaced the hard 90 deg. and 180 deg. pulses in order to suppress the H_2O line and excite the MbO_2 Val E11 resonance at –2.8 p.p.m. For the diffusion measurements, the acquisition parameters included the following: acquisition time, 64 ms; spectral width, 8012 Hz; data points, 1024. A typical spectrum took 24,576 scans, requiring approximately 30 min of signal accumulation. The free induction decays were zero filled to 4 k and multiplied by an exponential-Gaussian window function.

Previous reports have detailed the diffusion analysis based on a modified Bloch equation (Lin et al., 2007a; Lin et al., 2007b):

$$\frac{\partial \vec{M}(\vec{r},t)}{\partial t} = \pi \vec{M}(\vec{r},t) \times \vec{B}(\vec{r},t) - \frac{M_x \hat{i} + M_y \hat{j}}{T_2} - \frac{(M_z - M_0)\hat{k}}{T_1} + \nabla D(\vec{r}) \bullet \nabla \vec{M}(\vec{r},t) , \quad (1)$$

where γ is the magnetogyric ratio. The first three terms on the right correspond to the general Bloch equation; the last term, $=D\cdot\vec{M}$, reflects the effect of anisotropic diffusion (Torrey, 1956). Its solution, based on the NMR diffusion experiment, requires measurements of the echo amplitude $S(G)$ as a function of the applied field-gradient $G(t)$ (Price, 1997). For isotropic diffusion, the solution reduces to the following equation (Nicolay et al., 2001):

$$S(2\tau) = S(0)\exp(-\frac{2\tau}{T_2})\exp(-\gamma^2 D G^2 \delta^2 (\Delta - \frac{\delta}{3}) , \quad (2)$$

with the parameters specified as signal intensity at τ=0 [$S(0)$], signal intensity in an applied field G [$S(G)$], the applied field-gradient G, echo time τ, transverse relaxation time T_2, diffusion coefficient D, gradient pulse width δ, and gradient pulse interval Δ.

The following equation is then used to assess the relative contribution of free O_2 and Mb to the intracellular flux:

$$\frac{f_{O_2}^{Mb}}{f_{O_2}^{O_2}} = \frac{D_{Mb} C_{Mb}}{K_0 (P_{O_2} + P_{50})} , \quad (3)$$

where P_{O_2} = partial pressure of O_2, f_{O_2} = O_2 flux density, $f_{O_2}^{Mb}$ = O_2 flux density from Mb, $f_{O_2}^{O_2}$ O_2 flux density from free O_2, K_0 = Krogh's diffusion constant for free O_2, D_{Mb} = Mb diffusion coefficient, C_{Mb} = Mb concentration, $P_{50} = P_{O_2}$ that half saturates Mb, which reflects the O_2 binding affinity of Mb. When $f_{O_2}^{Mb}/f_{O_2}^{O_2} = 1$, Mb-facilitated O_2 and free O_2 contribute equally to the O_2 flux. The P_{O_2} corresponding to the condition $f_{O_2}^{Mb}/f_{O_2}^{O_2} = 1$ is defined as the equipoise diffusion P_{O_2}.

Statistical analysis

Statistical analysis used the Sigma Plot/Sigma Stat program (Systat Software, Point Richmond, CA, USA) and expressed the data as mean values ± standard deviation. Linear least-squares regression analysis of the individual data points determined the slopes, intercepts and correlation coefficients. Statistical significance was determined by two-tailed Student's t-test, $P<0.05$. All regression analyses used primary data points.

RESULTS

Fig. 1 shows a set of typical blood flow responses during six long apneas. MBF decreases progressively from 12–30 perfusion units during eupnea to 2–5 perfusion units by the end of 8–12-min apneas. The mean apneic MBF decreases to 46±10% of the mean eupneic MBF of 17.2±1.3 perfusion units. MBF during the first 20% of the apneic periods was 70±14% of mean eupneic MBF. During the final 10% of the apneic period but prior to the end-of-apnea hyperemia, the MBF falls to 31±8% of the mean eupneic MBF.

The change in MBF does not coincide precisely with the eupnea to apnea transition. MBF begins to decrease during and, sometimes, before the last breath of eupnea; MBF also starts to increase at the end of apnea prior to the first breath of eupnea.

A 90% reduction in MBF during apnea requires a $t_{1/2}$ of 1.9±1.2 min. At the start of the apnea to eupnea transition, the initial MBF rises with a $t_{1/2}$ of 0.2±0.04 min. Within the first minute, the MBF reaches a mean value of 83±13% of the preceding eupnea MBF. Table 1 summarizes the physiological data.

Fig. 2 shows the ^{1}H NMR spectra acquired during an 8 min episode of eupnea to apnea. With apnea, Mb releases O_2, as reflected by the emergence of the proximal histidyl $N_\delta H$ signal of deoxy-Mb at 76.0±0.09 p.p.m. The signal increases to a steady-state level within 4 min (Fig. 2a–h). With the onset of eupnea after this short breath

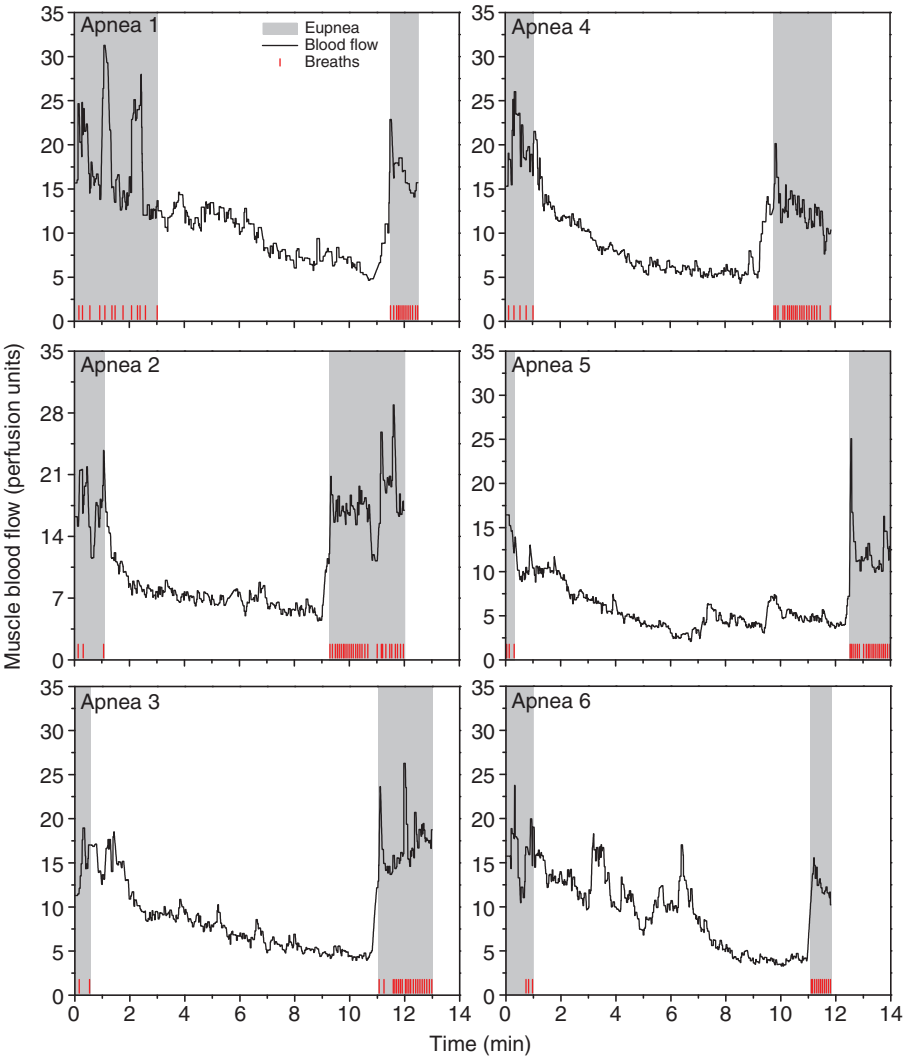

Fig. 1. Muscle blood flow (MBF) during six long apneas of an elephant seal. Apneic MBF decreases progressively but variably; occasional transient increases occur. At the end of apnea, MBF consistently increases prior to the first breath of eupnea. See Table 1 for a statistical summary. Note that MBF can also begin to decrease prior to the last breath of eupnea (apnea 1). Shaded area corresponds to eupnea period.

hold, the deoxy-Mb signal intensity decreases rapidly. Mb resaturates to its resting level within 1 min (Fig. 2n–o). An upfield peak also appears at 72–73 p.p.m., corresponding to the signal from the β subunits of deoxy-Hb (Tran et al., 1999). The deoxy-Hb signal continues to increase during apnea, even after Mb desaturation level has reached a steady-state level.

Fig. 3 traces the kinetics of Mb desaturation and resaturation during two apnea to eupnea cycles. During eupnea, ^{1}H NMR detects neither the deoxy-Mb nor the deoxy-Hb signal. At the onset of apnea, the deoxy-Mb signal appears as MbO_2 desaturates. MbO_2 releases about 20% of its oxygen store within 4 min. Mb maintains this desaturation level for rest of the apnea period. At the start of eupnea, both the deoxy-Mb and deoxy-Hb signals disappear as MBF returns to 83±5% of its eupnea level within 1 min to restore the vascular O_2 supply. Correspondingly, MbO_2 saturation recovers to about 95% of its resting level within 1 min. However, full recovery appears to require about 6 min.

During the eupneic interval shown in Fig. 3, Mb begins to desaturate during late eupnea as the respiratory rate slows and becomes intermittent prior to the onset of the next long apnea. Mb desaturation occurs under a constant tissue temperature of 35.1±0.4°C (Kreutzer et al., 1993).

Table 1. Muscle blood flow (MBF) during six long apneas

Apnea	Apneic duration (min)	Eupneic MBF (perfusion units)	Apneic MBF (% eupneic MBF)			Post-apneic MBF first min (% eupneic MBF)
			Initial 20%	Final 10%	Entire	
1	8.5	17.3	71	45	54	91
2	8.3	18.8	55	29	40	88
3	10.5	15.9	84	28	50	101
4	8.8	17.1	75	33	47	78
5	12.2	18.5	50	23	30	63
6	10.2	15.7	82	25	57	76
Mean±s.d.	9.8±1.5	17.2±1.3	70±14	31±8	46±10	83±13

Eupneic MBF was measured during the eupnea prior to the apnea. Apneic MBF during the final 10% of apnea was measured prior to the end-of-apnea increase in MBF.

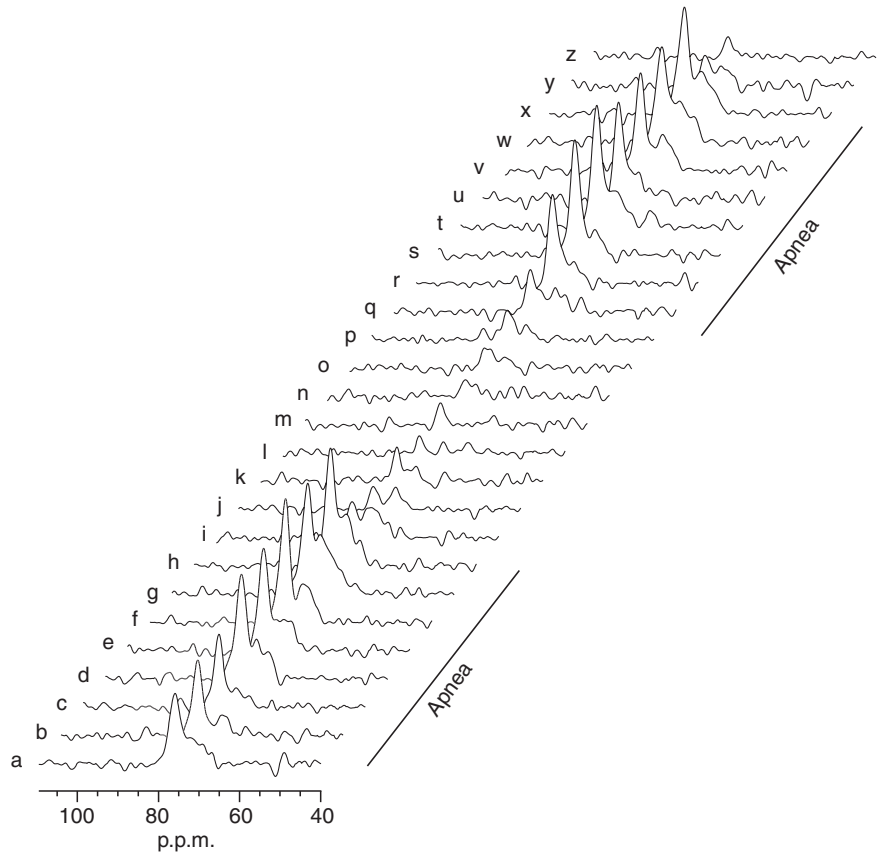

Fig. 2. ^{1}H NMR spectra of elephant seal muscle *in vivo* acquired during eupnea and apnea. ^{1}H spectra of the deoxy-Mb proximal histidyl $N_\delta H$ signal were recorded continuously for 25 min. Each spectrum required 1 min of signal averaging. During eupnea, the deoxy-Mb signal is not detected. Once apnea begins, the deoxy-Mb signal rises, indicating oxygen desaturation. As eupnea resumes, the signal decays rapidly, reflecting a restoration of the intracellular oxygen level.

Despite the rise and fall in MbO_2 saturation, which reflects the cellular P_{O_2}, the ^{31}P NMR spectra show no perturbation. Fig. 4 shows a typical bank of ^{31}P NMR spectra during eupnea to apnea cycles. Fig. 4a,b shows the ^{31}P spectra acquired during eupnea. Fig. 4c–f shows the corresponding signals during apnea. Fig. 4g–h shows the spectra during the second eupnea cycle. Under all conditions, the ^{31}P spectra remain unperturbed. The inorganic phosphate (P_i) chemical shift does not change, reflecting an unperturbed pH.

Fig. 5 shows the ^{1}H NMR spectra of the Val E11 signal of MbO_2 in seal muscle under different applied field gradients from 9.5, 23.8, 47.5 and 71.3 gauss cm^{-1}. As the field gradient increases, the Val E11 signal intensity decreases.

A natural logarithm plot of the MbO_2 signal intensity from seal muscle as a function of the square of the gradient strength applied along x direction yields a linear relationship with a regression coefficient (r^2>0.99) (Fig. 6). Given the linear equation, the analysis yields a Mb translational diffusion coefficient of $4.5\pm1.4\times10^{-7}$ cm^2 s^{-1} at 25°C.

Fig. 7 shows the relative contribution from Mb and free O_2 in transporting O_2 in the cell. The straight line depicts the contribution from free O_2 diffusion. The O_2 flux contribution from free O_2 diffusion reveals a linear dependence on P_{O_2} and has a slope that reflects the literature reported value for the Krogh's diffusion constant (K_0) of 2.5×10^{-5} ml O_2 cm^{-1} min^{-1} atm^{-1}. The O_2 flux from Mb shows a concentration-dependent response at a given D_{Mb} of 4.5×10^{-7} cm^2 s^{-1}. With a cytoplasmic Mb concentration of approximately 3.8 mmol l^{-1} and with a P_{50} assumed to be 1.5 mmHg at 25°C, the equipoise P_{O_2}, where Mb and free O_2 contribute equally, stands at 67 mmHg. Below 67 mmHg, the Mb contribution to cellular O_2 transport dominates.

DISCUSSION

Blood flow

During spontaneous breath holds of sleep apnea in seals, MBF gradually declines, punctuated by transient rises that have no association with movement or muscle fasciculation. At the end of apnea, MBF has fallen to approximately 30% of the eupneic flow

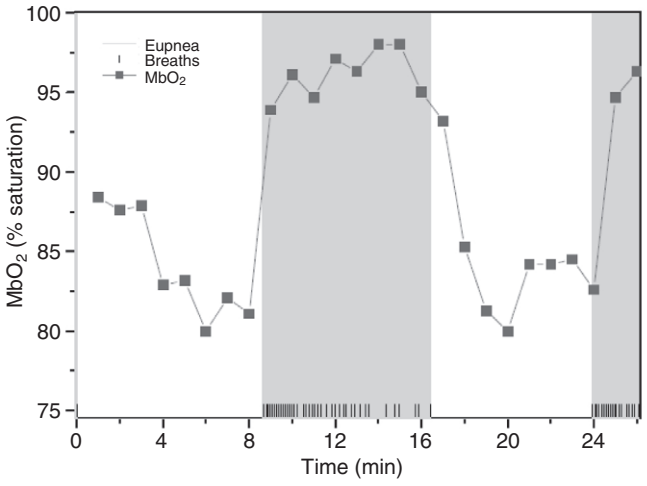

Fig. 3. The time course of MbO_2 desaturation–resaturation during apnea to eupnea cycles. The oxymyoglobin (MbO_2) saturation is derived from the calibrated proximal histidyl $N_\delta H$ signal of deoxy-Mb. MbO_2 saturation is plotted against time. Breaths are indicated by marks at the base of the graph. No deoxy-Mb signal is detectable during eupnea. During apnea, the MbO_2 desaturates by 20%, as calibrated from the external reference sample. Shaded area corresponds to eupnea period.

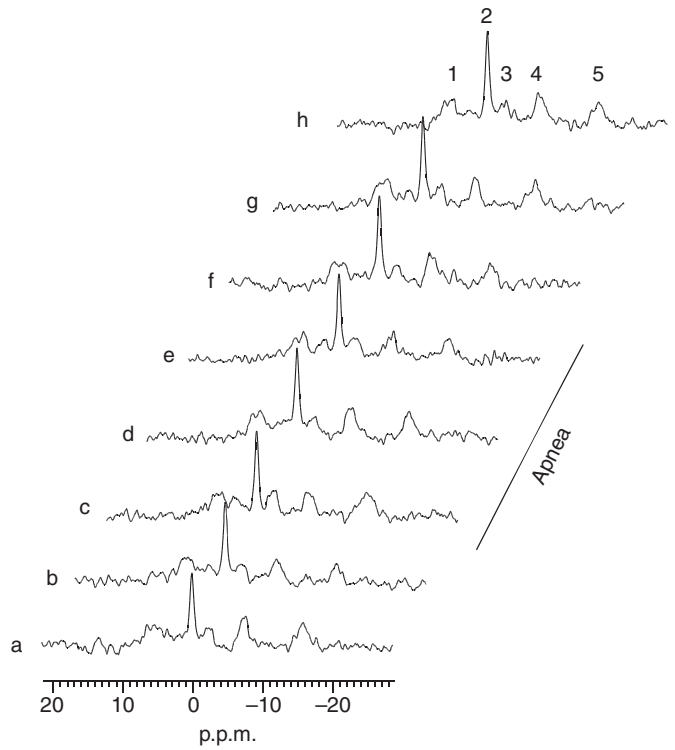

Fig. 4. Time course of ^{31}P NMR spectra of elephant seal muscle acquired *in vivo* during an apneic episode. The ^{31}P spectra were recorded continuously, each scan requiring 70 s of signal averaging. The spectra correspond to (a,b) eupneic state, (c–f) apneic state and (g,h) eupneic state. The ^{31}P signals exhibit no change during the eupnea to apnea transition. Peak 1 denotes P_i; peak 2, PCr; and peaks 3, 4 and 5, the γ, α and β signals of ATP, respectively.

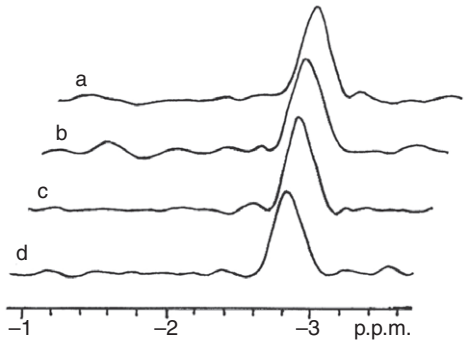

Fig. 5. ^{1}H NMR diffusion-weighted spectra of the Val E11 signal of MbO_2 from seal muscle at 25°C: A modified pulse PGSTE sequence detects the γ CH_3 Val E11 signal at –2.8 p.p.m. The peak intensity decreases as gradient field strength increases in the *x* direction: (a) 9.5 gauss cm^{-1} (1 gauss=10^4 tesla), (b) 23.8 gauss cm^{-1}, (c) 47.5 gauss cm^{-1} and (d) 71.3 gauss cm^{-1}.

rate. By contrast, during a breath hold in forced submersion experiments, MBF is severely reduced and, for the most part, is undetectable (Blix et al., 1983; Grinnell et al., 1942; Zapol et al., 1979). The inhomogeneous flow distribution during apnea agrees with the previously observed mosaic pattern of oxygenated/deoxygenated muscle (Scholander, 1940; Scholander et al., 1942; Blix et al., 1983). During the eupneic intervals between sleep apneas, MBF fluctuates; this is probably related to variations in respiratory rate and associated changes in heart rate and cardiac output during eupnea (Ponganis et al., 2006).

Oxygen supply

Synchronous with the fall in MBF, the O_2 level in the cell decreases rapidly to a reduced steady-state level, as reflected in the deoxy-Mb proximal histidyl $N_\delta H$ signal. In the control eupneic state, the undetectable deoxy-Mb signal indicates a cellular P_{O_2} well above the Mb P_{50}. Given the signal-to-noise ratio of the deoxy-Mb signal, NMR can detect the deoxy-Mb proximal histidyl $N_\delta H$ signal reflecting 10% MbO_2 desaturation. The resting eupneic state P_{O_2} must saturate at least 90% MbO_2, equivalent to above 18 mmHg based on the reported P_{50} of 2 mmHg at 35°C (Schenkman et al., 1997). As the respiratory rate starts to decrease during late eupnea, MbO_2 also begins to desaturate. Within 4 min of apnea, Mb has desaturated from the resting 3.8 mmol l^{-1} to 3.0 mmol l^{-1} MbO_2. Between 4 and 8 min of apnea, the MbO_2 does not desaturate further, indicating a constant cellular P_{O_2}. During apnea, the P_{O_2} has fallen to approximately 6 mmHg, corresponding to 80% MbO_2 saturation.

The returning oxygen at the transition from apnea to eupnea resaturates Mb more rapidly than the Mb desaturation during apnea. Within 1 min of the first breath, the deoxy-Mb signal diminishes significantly. MBF returns to 83±5% of the eupnea level whereas MbO_2 saturation recovers from about 80% to 90%. Full recovery of MbO_2 saturation to the control level appears to require an additional 5 min. The recovery of blood flow and cellular O_2 appears to follow a similar time course, although the slight mismatch at the initial phase of eupnea suggests a time lag in the appearance of a shortfall in O_2 delivery and a decrease in the intracellular O_2 level. Moreover, the recovery profile suggests a biphasic kinetics, which future experiments with improved time resolution of the deoxy-Mb detection must confirm.

The NMR spectra also show a signal from the β proximal histidyl $N_\delta H$ of deoxy-Hb, which appears on the shoulder of the deoxy-Mb peak. As blood flow decreases, HbO_2 saturation decreases, consistent with declining vascular P_{O_2}. During eupnea, the deoxy-Hb signal disappears accordingly.

Muscle temperature

The chemical shift of the deoxy-Mb signal reflects the temperature of the cellular environment, as calibrated in the study of isolated elephant seal Mb (Ponganis et al., 2002). During apnea, the intracellular temperature remains at 35.1±0.4°C. The deoxy-Hb signal also indicates a similar temperature. The results of the present study agree with pulmonary artery blood measurements during similar spontaneous apneas in young elephant seals, which also show an intravascular temperature of 36–37°C (Ponganis et al., 2006). These muscle temperatures are 1–2°C less than deep muscle temperatures in Weddell seals at rest but are consistent with lower temperatures in peripheral muscle and tissues of both humans and marine mammals (Irving and Hart, 1957; Ponganis et al., 1993b; Saltin et al., 1968; Sessler, 2000).

O_2 control of cellular respiration

Under resting eupneic conditions, the vascular O_2 supplies the cell with sufficient O_2 to saturate at least 90% of the MbO_2; otherwise, the NMR spectra would reveal a proximal histidyl $N_\delta H$ signal of deoxy-Mb. Throughout the entire apnea period, the cell operates under a P_{O_2} that saturates Mb to approximately 80%. However, no sign of hypoxemia appears. The ^{31}P PCr and ATP signals remain

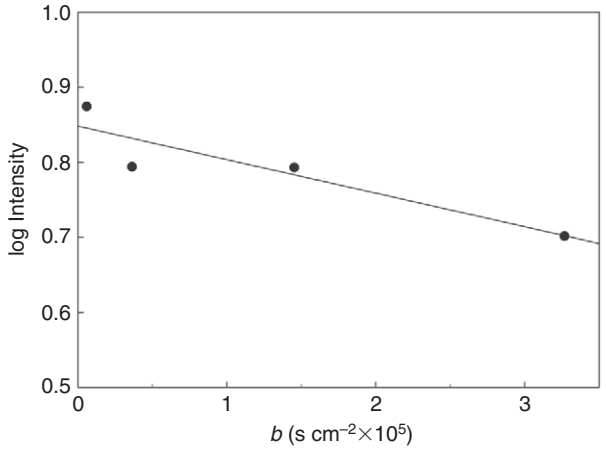

Fig. 6. Plots of the natural logarithm of the MbO_2 Val E11 peak intensity at 25°C as a function of b where $b=-\gamma^2G^2\delta^2(\Delta-\delta/3)$. The MbO_2 signals reveal decreasing intensity with each stepwise increase in gradient field strength applied along the x direction. The natural logarithm plot of signal intensity as a function b yields a linear relationship with a regression coefficient of r^2>0.99. Given the linear equation, the analysis has determined the Mb translational diffusion coefficient of $4.5\pm1.4\times10^{-7}$ cm^2 s^{-1} at 25°C.

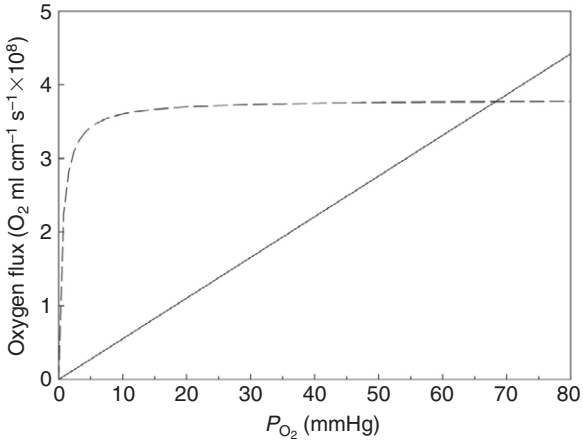

Fig. 7. Plots of Mb facilitated O_2 diffusion *vs* free O_2 flux as a function of P_{O_2} at 25°C. The equation $f_{O_2}^{O_2}=K_0P_{O_2}$ describes the linear rise of free O_2 flux with P_{O_2}. Krogh's diffusion coefficient, K_0, is the proportionality constant and the slope. The straight line shows the rate of change at a K_0 value of 2.52×10^{-5} ml O_2 cm^{-1} min^{-1} atm^{-1} at 23°C. The broken line graphs the equation $f_{O_2}^{Mb}=D_{Mb}C_{Mb}(P_{O_2}/P_{O_2}+P_{50})$, the Mb-facilitated O_2 diffusion as a function of P_{O_2}, P_{50}=1.5 mmHg (1 mmHg=0.133 kPa), C_{Mb}=3.8 mmol l^{-1} and $D_{Mb}=4.5\times10^{-7}$ cm^2 s^{-1}. The equipoise P_{O_2} 67 mmHg corresponds to the intersection of the two curves. Below 67 mmHg, the Mb contribution dominates.

constant throughout the entire eupnea to apnea cycles. The P_i chemical shift remains unaltered, reflecting a constant pH and rate of glycolysis. Indeed, sleep apnea experiments in seals have not detected any lactate washout (Castellini et al., 1994). All the metabolic indices do not reveal any tissue hypoxemia during apnea, despite the drop in cellular P_{O_2}.

However, the rate of oxygen uptake ($\dot{V}_{O_2}$) should remain at least constant during apnea, as the major energy expenditure incurred by muscle movement does not occur. If $\dot{V}_{O_2}$ remains constant, a decreasing vascular and intracellular O_2 supply that maintains the same $\dot{V}_{O_2}$ does not indicate that the O_2 level controls respiration during apnea.

$\dot{V}_{O_2}$ could potentially decrease as the O_2 delivery continues to fall during apnea. However, the intracellular P_{O_2} has reached a reduced steady-state level within 4 min, while MBF continues to decline. A constant intracellular P_{O_2} in the face of a falling $\dot{V}_{O_2}$ and MBF also argues against the simplistic notion of the O_2 level controlling $\dot{V}_{O_2}$ (Chung et al., 2005; Jue, 2004).

Mb contribution to O_2 transport

The regulation of $\dot{V}_{O_2}$ depends upon the free O_2 and Mb-facilitated O_2 flux in the cell. According to the Mb facilitated diffusion theory, as intracellular P_{O_2} falls, the oxygen-carrying capacity of Mb will enhance its flux contribution over free O_2. So, even if the O_2 level falls, the overall O_2 flux may still meet the $\dot{V}_{O_2}$ demand if the Mb-facilitated contribution to O_2 diffusion increases. This idea predicates usually on the hypothesis of a partially saturated Mb in resting muscle and requires a sufficiently rapid translational diffusion of Mb in the cell. Certainly, Mb does not appear significantly desaturated in the normoxic state in seal muscle as there is no sign of any deoxy-Mb signal. Moreover, recent studies have determined the Mb translational diffusion coefficient of 4.24×10^{-7} cm^2 s^{-1} in rat heart, which yields an equipoise P_{O_2} of 1.77 mmHg (Lin et al., 2007b). Below a P_{O_2} of 1.77 mmHg, the Mb-dependent contribution to the O_2 flux begins to dominate. In steady-state normoxic rat muscle, Mb doesn't appear to play a significant role in transporting cytoplasmic O_2 in the steady state (Lin et al., 2007a; Papadopoulos et al., 2001).

In contrast to the 0.19 mmol l^{-1} Mb concentration in rat heart, seal muscle contains a much higher concentration of Mb (4.5 g per 100 g tissue or approximately 3.8 mmol l^{-1} cytoplasmic Mb). Despite the 20× higher concentration in tissue, seal Mb still exhibits a translational diffusion of 4.5×10^{-7} cm^2 s^{-1} at 25°C. Given a free O_2 diffusion coefficient, K_0, of 2.5×10^{-5} ml O_2 cm^{-1} min^{-1}atm^{-1}, a P_{50} of 1.5 mmHg at 25°C and a Mb concentration of 3.8 mmol l^{-1}, the analysis yields an equipoise P_{O_2} of 67 mmHg. At physiological temperature of 37°C, K_0, P_{50} and D_{Mb} will increase to lower the equipoise P_{O_2} (Lin et al., 2007a).

During the intermittent breathing pattern of eupnea, venous P_{O_2} ranges between 34 and 71 mmHg (Stockard et al., 2007). At the start of apnea, average O_2 tension is approximately 59 mmHg. By 9 min of apnea, the mean venous P_{O_2} drops to 21 mmHg. Therefore, the calculated equipoise P_{O_2} is still much greater than the venous P_{O_2}. The eupnea to apnea transition does not correspond to any switch in intracellular O_2 transport as intracellular O_2 level falls. Mb plays a predominant role in transporting O_2 under all physiological conditions.

Transient *vs* steady-state levels of O_2

However, steady-state bioenergetics analysis misses the transient response that maintains the energetic homeostasis. At the start of apnea, Mb desaturates within 2 min by 10% of its control value. Within 4 min, Mb desaturates by 20% of the control value to the steady-state apneic value. Mb remains at 80% oxygen saturation throughout apnea. Given the assumption of no vascular O_2 contribution and a Mb concentration of 3.8 mmol l^{-1}, Mb desaturates at 190 μmol l^{-1} min^{-1} or about 3 μmol l^{-1} s^{-1}. The rate of Mb desaturation implies a resting muscle $\dot{V}_{O_2}$ of at least 3 μmol l^{-1} s^{-1}, consistent with the observed values in mammalian muscle (Blei et al., 1993; Chung et al., 2005). This leads to approximately 2 ml O_2 kg^{-1} muscle min^{-1} or 3 ml O_2 kg^{-1} muscle min^{-1} (based on

a 20% desaturation of 4.5 g Mb 100 g^{-1} or 60 ml O_2 kg^{-1} over 4 min). Indeed, the $\dot{V}_{O_2}$ estimate matches the lower range of resting $\dot{V}_{O_2}$ observed in the latissimus dorsi muscle of diving Weddell seals (Guyton et al., 1995) and suggests that Mb supplies the transient O_2 need at the beginning of apnea, when vascular O_2 supply can no longer meet the change in O_2 demand (Castellini et al., 1992).

Within 1 min of the apnea to eupnea transition, the vascular O_2 restores Mb almost to the control saturation level at a rate of 760 μmol l^{-1} min^{-1} or 13 μmol l^{-1} s^{-1}, about 4.3× faster than the Mb desaturation rate at the beginning of apnea. The difference in Mb desaturation and resaturation kinetics parallels the change in blood flow. Blood flow falls to 30% of its normoxic level within 5 min of apnea and recovers to its basal level within 1 min of eupnea. The oxygen restoration profile parallels the end tidal P_{O_2} response in free-diving Weddell seals (Ponganis et al., 1993a).

If the MBF and $\dot{V}_{O_2}$ always match, as some researchers have asserted, then the eupneic and apneic $\dot{V}_{O_2}$ must differ by at least a factor of five as eupneic MBF (MBF_E)~2×MBF_A (Table 1) but ($O^E_{2capillary}$–O^E_{2cell})=2.7($O^A_{2capillary}$–O^A_{2cell}) (*vide infra*). The relationship in the relative change in eupneic *vs* apneic $\dot{V}_{O_2}$ is as follows:

$$\frac{\dot{V}^E_{O_2}}{\dot{V}^A_{O_2}} = \frac{(O^E_{2capillary} - O^E_{2cell})}{(O^A_{2capillary} - O^A_{2cell})} \frac{MBF_E}{MBF_A}\ , \qquad (4)$$

where $\dot{V}^E_{O_2}/\dot{V}^A_{O_2}$ = ratio of eupneic to apneic $\dot{V}_{O_2}$, $O^E_{2capillary}$–O^E_{2cell})/($O^A_{2capillary}$–O^A_{2cell}) = ratio of eupneic to apneic O_2 gradient, (MBF_E)/(MBF_A) = ratio of eupneic to apneic MBF. The rapid MBF kinetics, as reflected in the MbO_2 resaturation, should match the rising $\dot{V}_{O_2}$. However, during post-exercise, when the $\dot{V}_{O_2}$ falls, studies have also observed a rapid MbO_2 resaturation kinetics (Chung et al, 2006). A rapid resaturation kinetics with either rising or falling $\dot{V}_{O_2}$ argues against a tight match between MBF and $\dot{V}_{O_2}$.

Alternatively, the rapid MbO_2 resaturation and MBF recovery kinetics reflect a two-step process. The recovering MBF at the start of eupnea supplies O_2 to the cell and resaturates Mb. This rate of O_2 resaturation (13 μmol l^{-1} s^{-1}) far exceeds the eupneic $\dot{V}_{O_2}$ of 3 μmol l^{-1} s^{-1}. In essence, the O_2 supply alone does not control $\dot{V}_{O_2}$ during the apnea to eupnea transition, and MBF has an overcapacity in delivering O_2 supply above the cellular need, as observed in the functional magnetic resonance imaging of brain cell activation (Hyder et al., 2001).

Mb as an O_2 buffer

In muscle, the initiation of contraction increases the energy demand, which momentarily outstrips the vascular supply of O_2. Such a transient mismatch leans on Mb to buffer the O_2 deficit. Indeed, Mb appears to serve that role at the start of muscle contraction; it desaturates to a steady-state within ~30 s (Chung et al., 2005).

During the 8–12 min apnea to eupnea cycle, seal muscle does not contract or move. So, the muscle energy demand has not increased to drive Mb desaturation. Instead, vascular O_2 delivery has decreased. MBF declines to 50% of its final value within 2 min and 90% of its final value in approximately 4 min. The correlation of Mb desaturation kinetics with MBF indicates that the transient mismatch of O_2 supply and demand during the eupnea to apnea transition triggers the release of O_2 from the Mb. As observed at the initiation of muscle contraction, Mb serves as an O_2 buffer during a transient mismatch of cellular supply and demand for O_2.

The equipoise P_{O_2} analysis, based on translational diffusion of Mb, indicates that Mb has a predominant role to facilitate O_2 transport in the cell under both eupnea and apnea. This would suggest that Mb plays a key role in O_2 buffering only at the beginning of apnea.

Implication of O_2 gradient on apnea $\dot{V}_{O_2}$

The P_{O_2} reflected in the Mb saturation data and previously measured apneic venous P_{O_2} data allow assessment of the blood-to-muscle O_2 gradient during sleep apnea (Stockard et al., 2007). During early apnea, Mb saturation, as reflected in the deoxy-Mb signal, declines to 80%. Assuming a Mb P_{50} of 2 mmHg at 35°C, 80% saturation would correspond to a tissue P_{O_2} of approximately 6 mmHg. A change from 90% to 80% Mb saturation represents a P_{O_2} decline from 18 to 6 mmHg inside the cell (Araki et al., 1983; Schenkman et al., 1997). Venous P_{O_2}, on average, declines from 59 mmHg at the start of apnea to 52 mmHg by 3 min into apnea (Stockard et al., 2007). Using venous P_{O_2} as an estimate of the end capillary mean P_{O_2}, the blood-to-muscle O_2 gradient will remain about the same at the start of apnea (41 mmHg) and at 3 min into apnea (46 mmHg).

However, as apnea progresses, the venous P_{O_2} continues to decline, reaching a value of 21 mmHg by 9 min into apnea (Stockard et al., 2007). This decline in venous P_{O_2} is reflected by the appearance of the deoxy-Hb signal in the ^1H spectra. However, intracellular P_{O_2} remains at 6 mmHg as apnea progresses. Consequently, the blood-to-muscle O_2 gradient decreases by a factor of 2.7 from 41 mmHg at the start of apnea to 15 mmHg at 9 min into apnea.

Fick's diffusion law indicates that as the O_2 gradient narrows, $\dot{V}_{O_2}$ must decrease. The narrowing of the O_2 gradient implies that $\dot{V}_{O_2}$ falls during apnea. Otherwise, P_{O_2} should continue to fall to maintain the O_2 gradient that continues a proper O_2 flux to support a constant $\dot{V}_{O_2}$. A similar conclusion emerges from the analysis of MBF, arterial–venous difference in O_2 and $\dot{V}_{O_2}$:

$$\dot{V}_{O_2} = (O_{2arterial} - O_{2venous}) \times MBF\,. \qquad (5)$$

As apnea progresses, the arterial–venous O_2 difference collapses (Stockard et al., 2007); however, MBF also decreases. Consequently, $\dot{V}_{O_2}$ must also decrease. As no muscle movement occurs during apnea, the reduced $\dot{V}_{O_2}$ implies that the energy demand, presumably with ATP-dependent ion transporters, must downregulate.

By contrast, during complete muscle ischemia in head-immersed Pekin ducks (*Anas platyrhynchos*), the ATP turnover rate in pectoral muscle is maintained at pre-submersion levels through depletion of the Mb oxygen store, PCr breakdown and increased glycolysis (lactate accumulation) (Stephenson and Jones, 1992). This difference in muscle metabolic response between sleep apnea in the elephant seal and head immersion in the Pekin duck may, of course, be secondary to the physical (restraint/struggling) and physiological differences between a spontaneous apnea of an elephant seal and the forced head immersion of a duck. It is notable that paralysis of the muscle in the head-immersed duck resulted in no detectable PCr breakdown or change in intracellular pH during immersion. Presumably, the O_2 store of Mb was adequate for energy demand under these conditions. Complete depletion of the O_2 reservoir of Mb over the duration of the immersion would have resulted in an ATP turnover rate that was only 10% of that of a non-paralyzed muscle of a restrained duck at rest.

It should be noted that declines in muscle $\dot{V}_{O_2}$ in relation to low MBF have also been observed in other species (Duran and Renkin, 1974; Gutierrez et al., 1988; Mizuno et al., 2003). Thus, the predicted decline in muscle $\dot{V}_{O_2}$ during sleep apnea in the elephant seal does not appear to represent a unique mechanism of metabolic depression exclusive to diving animals. Although bradycardia and decreased tissue blood flow during a breath hold will reduce metabolic rate in muscle (above) and other organs (Scholander, 1940; Scholander et al., 1942), all data of elephant seals during sleep apnea indicate that most metabolic processes in other tissues continue (Ponganis

et al., 2006). Indeed, the apneic $\dot{V}_{O_2}$ and cardiac output mirror resting-state values. During eupnea, the increased $\dot{V}_{O_2}$ and cardiac output reflect the increased respiratory costs and increased O_2 uptake/consumption associated with increased blood flow to organs/muscle. Rather than considering sleep apnea as a hypometabolic state, it is more appropriate to consider the eupneic period as an elevated metabolic state. This is the same conclusion reached by Castellini and Zenteno-Savin in an allometric analysis of seal heart rates (Castellini and Zenteno-Savin, 1997).

In addition, the present study's experimental data and the previously estimated blood O_2 contribution to metabolic rate during sleep apnea (Stockard et al., 2007) do not provide any evidence of whole-body hypometabolism. Using the blood O_2 depletion during sleep apnea in these seals in a prior study and the net muscle O_2 depletion (about 250 ml O_2) determined in the present study (20% decline in Mb saturation at a concentration of 45 g kg^{-1} muscle tissue with muscle approximately 30% of a 70 kg body mass), the analysis yields a combined blood and muscle O_2 store depletion rate during a typical 7 min apnea of 4.7 ml O_2 kg^{-1} body mass min^{-1} (Stockard et al., 2007). As the lung O_2 store in seals is only about 5% of the total O_2 store and neither lactate nor PCr shows any change, this combined blood and muscle O_2 depletion rate should closely approximate the actual metabolic rate during the breath-hold period. However, this value is still 26% greater than the Kleiber-predicted resting metabolic rate for a 70 kg mammal at rest (Kleiber, 1961; Kleiber and Rogers, 1961).

PCr kinetics and $\dot{V}_{O_2}$

Throughout eupnea and apnea, the PCr and ATP levels remain constant, despite the dynamic changes in intracellular P_{O_2} and $\dot{V}_{O_2}$. Certainly, the unchanging PCr/ATP ratio indicates that the tissue does not suffer from any ischemia as MBF decreases to 30% of the eupneic level and vascular P_{O_2} drops from about 60 to 21 mmHg. During apnea, metabolism can still rely on oxidative phosphorylation. The resultant CO_2 from oxidative metabolism can alter respiratory drive as well as sleep structure (Milsom et al. 1996; Skinner and Milsom, 2004; Stephenson, 2005). Indeed, marine and terrestrial mammals appear to have similar hypercarbic chemosensitivity but do not have the same thresholds as a result of contrasting blood buffering capacity.

The presence of a non-limiting oxidative phosphorylation addresses a long-standing postulate that envisions PCr breakdown supplementing glycolysis during a dive to compensate for the presence of hypoxemia (Hochachka and McClelland, 1997). During sleep apnea, this does not occur because muscle tissue hypoxemia does not exist. From a conventional vantage, blood flow and intracellular P_{O_2} fall correspondingly to maintain an O_2 gradient that sustains the $\dot{V}_{O_2}$. Oxygen delivery dynamically matches the oxygen demand. The release of O_2 from the Mb then provides a temporary source of O_2 as the gradient adjusts. Once the gradient has adjusted, Hb can provide an adequate flux of O_2 for cellular respiration. With adequate delivery of O_2, no deficit in oxidative ATP generation exists. Creatine kinase does not need to mobilize PCr to buffer any ATP loss. The cell can still rely on aerobic metabolism. The PCr level should then not change.

But as the gradient narrows later on during apnea and blood flow declines to 30% the eupneic level, $\dot{V}_{O_2}$ must fall by a factor of five, well below the value at the start of apnea. Yet no signs of tissue hypoxia or ischemia, as measured by elevated lactate production, appear. Either muscle $\dot{V}_{O_2}$ can decrease significantly without producing any tissue hypoxia or the efficiency of energy utilization has improved dramatically or the current measurements do not adequately detect the shift in metabolic regulation (Whalen et al., 1974).

Recent studies have suggested that experimental measurements might not accurately track the transient metabolic response. Standard measurements of PCr with ^{31}P NMR show no change in the PCr intensity ascribed to a single twitch. Yet, NMR techniques tailored to capture metabolic transients show a significant use of ATP and PCr per contraction cycle, far greater than the conventional assessments reported in the literature (Chung et al., 1998). Such metabolic transients raise questions about the fluxes that maintain the cellular bioenergetics and suggest a dynamic control of energy flux from glycogen, glucose and respiration as proposed in the glycogen shunt model (Shulman and Rothman, 2001). This model does not restrict lactate as only a metabolic end product reflecting hypoxemia or ischemia. Instead, studies have shown that lactate can become oxidized to serve as a direct mitochondrial precursor for oxidative phosphorylation (Brooks et al., 1999). Conventional ^{31}P NMR and metabolic measurements would miss these dynamic fluxes.

Finally, if the $\dot{V}_{O_2}$ has decreased dramatically during apnea, then the returning O_2 during the apnea to eupnea transition will restore the O_2 and the $\dot{V}_{O_2}$ to the higher eupneic level. The postulated $\dot{V}_{O_2}$ recovery from a lower rate still shows no corresponding change in PCr. Thus, PCr recovery rate does not always reflect $\dot{V}_{O_2}$ recovery or oxidative capacity (Chung et al., 2006; Foley and Meyer, 1993).

Indeed, the metabolic adaptation in seal muscle during a breath hold as reflected in the eupnea to apnea transition indicates a complex relationship between $\dot{V}_{O_2}$ and PCr, which requires additional investigation.

Conclusion

In conclusion, NMR spectroscopy has provided new insights into Mb function and blood-to-muscle O_2 transfer during the breath holds of sleeping elephant seals. Aerobic metabolism in muscle is maintained, despite the fall in intracellular and vascular O_2. PCr and ATP levels do not change. As MBF declines during apnea, Mb buffers the initial loss of the O_2 supply by releasing its O_2 store. MbO_2 desaturates quickly to a steady-state level, which reflects an adjustment of the O_2 gradient from the vasculature to the cell. No switch from free to Mb-facilitated O_2 diffusion occurs, as under all physiological conditions the equipoise analysis of Mb translation diffusion asserts a predominant role for Mb as the intracellular O_2 transporter.

Despite the continuing decline in the vascular P_{O_2} during sleep apnea, the intracellular P_{O_2} of muscle does not change significantly after its initial fall. A constant intracellular P_{O_2}, in association with (1) a declining vascular P_{O_2} and a narrowing O_2 gradient, (2) constant PCr and ATP levels, and (3) a lack of lactate accumulation, implies a downregulation of ATP demand. Such declines in muscle metabolic rate in relation to decreased MBF have been observed in other species. Even with such regulation of muscle metabolic rate, sleep apnea should not be considered a hypometabolic state. The combined depletion of blood and muscle O_2 stores during the breath hold yields a whole-body $\dot{V}_{O_2}$ greater than the Kleiber-predicted resting metabolic rate.

These findings during sleep apnea contrast with those during forced submersion (severe bradycardia/vasoconstriction, complete circulatory isolation of muscle and depletion of muscle O_2, and conservation of blood O_2 for the heart and brain). During dives, we suspect that the intensity and magnitude of these physiological and metabolic responses will range between these two extremes, dependent on the nature of a given dive and the associated reduction in heart rate. As Scholander emphasized, O_2 consumption and the rate of blood O_2 depletion will ultimately depend on the heart rate

response (Scholander, 1940). Similarly, the role of the high Mb concentrations in seal muscle (facilitation of O_2 diffusion *vs* an O_2 store) will also be dependent on the intensity of the cardiovascular response during a dive. Although our analyses predict that basal muscle $\dot{V}_{O_2}$ during sleep apnea decreases in relation to even moderate declines in MBF, muscle $\dot{V}_{O_2}$ during dives will probably be most dependent on the locomotory workload of muscle.

We gratefully acknowledge the support by UCSD Academic Senate Grant RY253S, a UC MRIF Award (P.J.P.), NSF grant IBN 00-78540 (P.J.P., T.J.) and by NIH Grant GM 57355 (T.J.). We also thank D. Levenson and numerous volunteers/assistants for care and training of the seals, Dr R. Shadwick for use of his computer A-D interface and Dr K. Ponganis for graphics. A special note of thanks extends to Dr Lawrence Litt, who facilitated the protocol through the UCSF Committee on Animal Research. Without Dr Litt's gracious help, some of the NMR experiments would not have been possible.

REFERENCES

Andrews, R. D., Jones, D. R., Williams, J. D., Thorson, P. H., Oliver, G. W., Costa, D. P. and Le Boeuf, B. J. (1997). Heart rates of Northern elephant seals while diving at sea and resting on the beach. *J. Exp. Biol.* **200**, 2083-2095.

Araki, R., Tamura, M. and Yamazaki, I. (1983). The effect of intracellular oxygen concentration on lactate release, pyridine nucleotide reduction, and respiration rate in the rat cardiac tissue. *Circ. Res.* **53**, 448-455.

Blei, M., Conley, K. E. and Kushmerick, M. J. (1993). Separate measures of ATP utilization and recovery in human skeletal muscle. *J. Physiol.* **465**, 203-222.

Blix, A. S., Elsner, R. W. and Kjekhus, J. K. (1983). Cardiac output and its distribution through capillaries and A-V shunts in diving seals. *Acta Physiol. Scand.* **118**, 109-116.

Brooks, G. A., Dubouchaud, H., Brown, M., Sicurello, J. P. and Butz, C. E. (1999). Role of mitochondrial lacate dehydrogenase and lactate oxidation in the intracellular lactate shuttle. *Proc. Natl. Acad. Sci. USA* **96**, 1129-1134.

Castellini, M. A. and Zenteno-Savin, T. (1997). Heart rate scaling with body mass in pinnipeds. *Mar. Mamm. Sci.* **13**, 149-155.

Castellini, M. A., Costa, D. P. and Huntley, A. (1986). Hematocrit variation during sleep apnea in elephant seal pups. *Am. J. Physiol.* **251**, R429-R431.

Castellini, M. A., Kooyman, G. L. and Ponganis, P. J. (1992). Metabolic rates of freely diving Weddell seals: correlations with oxygen stores, swim velocity and diving duration. *J. Exp. Biol.* **165**, 181-194.

Castellini, M. A., Milsom, W. K., Berger, R. J., Costa, D. P., Jones, D. R., Castellini, J. M., Rea, L. D., Bharma, S. and Harris, M. (1994). Patterns of respiration and heart rate during wakefulness and sleep in elephant seal pups. *Am. J. Physiol.* **266**, R863-R869.

Chung, Y., Sharman, R., Carlsen, R., Unger, S. W., Larson, D. and Jue, T. (1998). Metabolic fluctuation during a muscle contraction cycle. *Am. J. Physiol.* **274**, C846-C852.

Chung, Y., Molé, P. A., Sailasuta, N., Tran, T. K., Hurd, R. and Jue, T. (2005). Control of respiration and bioenergetics during muscle contraction. *Am. J. Physiol.* **288**, C730-C738.

Chung, Y., Molé, P. A., Tran, T. K., Sailasuta, N., Masuda, K., Hurd, R. and Jue, T. (2006). Muscle bioenergetics during exercise recovery. *Med. Sci. Sports. Med.* 38, (11), S14.

Duran, W. N. and Renkin, E. M. (1974). Oxygen consumption and blood flow in resting mammalian skeletal muscle. *Am. J. Physiol.* **226**, 173-177.

Elsner, R. W., Franklin, D. L. and VanCitters, R. L. (1964). Cardiac output during diving in an unrestrained sea lion. *Nature* **202**, 809-810.

Foley, J. M. and Meyer, R. A. (1993). Energy cost of twitch and tetanic contractions of rat muscle estimated *in situ* by gated 31P NMR. *NMR Biomed.* **6**, 32-38.

Glover, G. H. and Schneider, E. (1991). Three-point Dixon technique for true water/fat decomposition with Bo inhomogeneity correction. *Magn. Reson. Med.* **18**, 371-383.

Grinnell, S. W., Irving, L. and Scholander, P. F. (1942). Experiments on the relation between blood flow and heart rate in the living seal. *J. Cell. Comp. Physiol.* **19**, 341-350.

Gutierrez, G., Pohil, R. J. and Strong, R. (1988). Effect of flow on O_2 consumption during progressive hypoxemia. *J. Appl. Physiol.* **65**, 601-607.

Guyton, G. P., Stanek, K. S., Schneider, R. C., Hochachka, P. W., Hurford, W. E., Zapol, D. G., Liggins, G. C. and Zapol, W. M. (1995). Myoglobin saturation in free-diving Weddell seals. *J. Appl. Physiol.* **79**, 1148-1155.

Hochachka, P. W. and McClelland, G. B. (1997). Cellular metabolic homeostasis during large-scale change in ATP turnover rates in muscles. *J. Exp. Biol.* **200**, 381-386.

Hyder, F., Kida, I., Behar, K. L., Kennan, R. P., Maciejewski, P. K. and Rothman, D. L. (2001). Quantitative functional imaging of the brain: towards mapping neuronal activity by BOLD fMRI. *NMR Biomed.* **14**, 413-431.

Irving, L. and Hart, J. S. (1957). The metabolism and insulation of seals as bare-skinned mammals in cold water. *Can. J. Zool.* **35**, 498-511.

Jue, T. (2004). Bioenergetics implication of metabolic fluctuation during muscle contraction. In *Metabolomics by in vivo NMR* (ed. R. G. Shulman and D. L. Rothman), pp. 104-117. Chichester: John Wiley.

Kleiber, M. (1961). *Fire of Life.* New York: John Wiley & Sons.

Kleiber, M. and Rogers, T. (1961). Energy metabolism. *Annu. Rev. Physiol.* **23**, 5-36.

Kreutzer, U. and Jue, T. (1995). Critical intracellular oxygen in the myocardium as determined with the 1H NMR signal of myoglobin. *Am. J. Physiol.* **268**, H1675-H1681.

Kreutzer, U., Wang, D. S. and Jue, T. (1992). Observing the ^{1}H NMR signal of the myoglobin Val-E11 in myocardium: an index of cellular oxygenation. *Proc. Natl. Acad. Sci. USA* **89**, 4731-4733.

Kreutzer, U., Chung, Y., Butler, D. and Jue, T. (1993). ^{1}H-NMR characterization of the human myocardium myoglobin and erythrocyte hemoglobin signals. *Biochim. Biophys. Acta* **1161**, 33-37.

Kreutzer, U., Mekhamer, Y., Tran, T. K. and Jue, T. (1998). Role of oxygen in limiting respiration in the *in situ* myocardium. *J. Mol. Cell Cardiol.* **30**, 2651-2655.

Le Boeuf, B. J., Crocker, D. E., Grayson, J., Gedamke, J., Webb, P. M., Blackwell, S. B. and Costa, D. P. (2000). Respiration and heart rate at the surface between dives in northern elephant seals. *J. Exp. Biol.* **203**, 3265-3274.

Lin, P. C., Kreutzer, U. and Jue, T. (2007a). Anisotropy and temperature dependence of myoglobin translational diffusion in myocardium: implication on oxygen transport and cellular architecture. *Biophys. J.* **92**, 2608-2620.

Lin, P. C., Kreutzer, U. and Jue, T. (2007b). Myoglobin translational diffusion in myocardium and its implication on intracellular oxygen transport. *J. Physiol.* **578**, 595-603.

Masuda, K., Truscott, K., Lin, P. C., Kreutzer, U., Chung, Y., Sriram, R. and Jue, T. (2008). Determination of myoglobin concentration in blood-perfused tissue. *Eur. J. Appl. Physiol.* **104**, 41-48.

Milsom, W., Castellini, M., Harris, M., Castellini, J., Jones, D., Berger, R., Bahrma, S., Rea, L. and Costa, D. (1996). Effects of hypoxia and hypercapnia on patterns of sleep-associated apnea in elephant seal pups. *Am. J. Physiol.* **271**, R1017-R1024.

Mizuno, M., Kimura, Y., Iwakawa, T., Oda, K., Ishii, K., Ishiwata, K., Nakamura, Y. and Muraoka, I. (2003). Regional differences in blood flow and oxygen consumption in resting muscle and their relationship during recovery from exhaustive exercise. *J. Appl. Physiol.* **95**, 2204-2210.

Morris, G. A. and Freeman, R. (1978). Selective excitation in Fourier transform nuclear magnetic resonance. *J. Magn. Reson.* **29**, 433-462.

Nicolay, K., Braun, K. P., Graaf, R. A., Dijkhuizen, R. M. and Kruiskamp, M. J. (2001). Diffusion NMR spectroscopy. *NMR Biomed.* **14**, 94-111.

Papadopoulos, S., Endeward, V., Revesz-Walker, B., Jurgens, K. D. and Gros, G. (2001). Radial and longitudinal diffusion of myoglobin in single living heart and skeletal muscle cells. *Proc. Natl. Acad. Sci. USA* **98**, 5904-5909.

Ponganis, P. J., Kooyman, G. L. and Castellini, M. A. (1993a). Determinants of the aerobic dive limit of Weddell seals: analysis of diving metabolic rates, postdive end tidal pO_2's, and blood and muscle oxygen stores. *Physiol. Zool.* **66**, 732-749.

Ponganis, P. J., Kooyman, G. L., Castellini, M. A., Ponganis, E. P. and Ponganis, K. V. (1993b). Muscle temperature and swim velocity profiles during diving in a Weddell seal, *Leptonychotes weddellii*. *J. Exp. Biol.* **183**, 341-346.

Ponganis, P. J., Kreutzer, U., Sailasuta, N., Knower, T., Hurd, R. and Jue, T. (2002). Detection of myoglobin desaturation in *Mirounga angustirostris* during apnea. *Am. J. Physiol. Regul. Integr. Comp. Physiol.* **282**, R267-R272.

Ponganis, P. J., Stockard, T. K., Levenson, D. H., Berg, L. and Baranov, E. A. (2006). Cardiac output and muscle blood flow during rest-associated apneas of elephant seals. *Comp. Biochem. Physiol.* **144**, 105-111.

Price, W. S. (1997). Pulsed-field gradient nuclear magnetic resonance as a tool for studying translational diffusion.1: basic theory. *Concepts Magn. Reson.* **9**, 299-336.

Reynafarje, B. (1963). Simplified method for the determination of myoglobin. *J. Lab. Clin. Med.* **61**, 138-145.

Saltin, B., Gagge, A. P. and Stolwijk, J. A. J. (1968). Muscle temperature during submaximal exercise in man. *J. Appl. Physiol.* **25**, 679-688.

Schenkman, K. A., Marble, D. R., Burns, D. H. and Feigl, E. O. (1997). Myoglobin oxygen dissociation by multiwavelength spectroscopy. *J. Appl. Physiol.* **82**, 86-92.

Scholander, P. F. (1940). Experimental investigations on the respiratory function in diving mammals and birds. *Hvalradets. Skr.* **22**, 1-131.

Scholander, P. F., Irving, L. and Grinnell, S. W. (1942). Aerobic and anaerobic changes in seal muscles during diving. *J. Biol. Chem.* **142**, 431-440.

Sessler, D. I. (2000). Perioperative heat balance. *Anesthesiology* **92**, 578-596.

Shulman, R. G. and Rothman, D. L. (2001). The 'glycogen shunt' in exercising muscle: a role for glycogen in muscle energetics and fatigue. *Proc. Natl. Acad. Sci. USA* **98**, 457-461.

Skinner, L. A. and Milsom, W. K. (2004). Respiratory chemosensitivity during wake and sleep in harbour seal pups (*Phoca vitulina richardsii*). *Physiol. Biochem. Zool.* **77**, 847-863.

Stejskal, E. O. and Tanner, J. E. (1965). Spin diffusion measurements: spin echoes in the presence of a time-dependent field gradient. *J. Chem. Phys.* **42**, 288-292.

Stephenson, R. (2005). Physiological control of diving behaviour in the Weddell seal *Leptonychotes weddellii*: a model based on cardiorespiratory control theory. *J. Exp. Biol.* **208**, 1971-1991.

Stephenson, R. and Jones, D. R. (1992). Metabolic responses to forced dives in Pekin duck measured by indirect calorimetry and 31P-MRS. *Am. J. Physiol.* **263**, R1309-R1317.

Stockard, T. K., Levenson, D. H., Berg, L., Fransiolo, J. R., Baranov, E. A. and Ponganis, P. J. (2007). Blood oxygen depletion during rest-associated apneas of northern elephant seals (*Mirounga angustirostris*). *J. Exp. Biol.* **210**, 2607-2617.

Torrey, H. C. (1956). Bloch equations with diffusion terms. *Phys. Rev.* **104**, 563-565.

Tran, T. K., Sailasuta, N., Kreutzer, U., Hurd, R., Chung, Y., Mole, P., Kuno, S. and Jue, T. (1999). Comparative analysis of NMR and NIRS measurements of intracellular PO_2 in human skeletal muscle. *Am. J. Physiol.* **276**, R1682-R1690.

Whalen, W. J., Nair, P., Buerk, D. and Thuning, C. A. (1974). Tissue P_{O_2} in normal and denervated cat skeletal muscle. *Am. J. Physiol.* **227**, 1221-1225.

Zapol, W. M., Liggins, G. C., Schneider, R. C., Qvist, J., Snider, M. T., Creasy, R. K. and Hochachka, P. W. (1979). Regional blood flow during simulated diving in the conscious Weddell seal. *J. Appl. Physiol.* **47**, 968-973.